LASER INTERFEROMETER GRAVITATIONAL WAVE OBSERVATORY
- LIGO -
CALIFORNIA INSTITUTE OF TECHNOLOGY
MASSACHUSETTS INSTITUTE OF TECHNOLOGY

Technical Note **LIGO-T11XXXXX–vX** 2020/06/18

Optical Refrigeration for LIGO Instruments

S. Schulz
Mentors: R. Adhikari, Y. Drori, C. Wipf

California Institute of Technology
LIGO Project, MS 18-34
Pasadena, CA 91125
Phone (626) 395-2129
Fax (626) 304-9834
E-mail: info@ligo.caltech.edu

Massachusetts Institute of Technology
LIGO Project, Room NW22-295
Cambridge, MA 02139
Phone (617) 253-4824
Fax (617) 253-7014
E-mail: info@ligo.mit.edu

LIGO Hanford Observatory
Route 10, Mile Marker 2
Richland, WA 99352
Phone (509) 372-8106
Fax (509) 372-8137
E-mail: info@ligo.caltech.edu

LIGO Livingston Observatory
19100 LIGO Lane
Livingston, LA 70754
Phone (225) 686-3100
Fax (225) 686-7189
E-mail: info@ligo.caltech.edu

http://www.ligo.caltech.edu/

1 Introduction

1.1 Motivation

Gravitational waves (GWs) are ripples in spacetime which propagate at the speed of light and are caused by the acceleration of massive objects. Their existence was predicted in 1916 by Albert Einstein when he developed the general theory of relativity [1]. The Laser Interferometer Gravitational-wave Observatory (LIGO) is a national facility for GW research consisting of two interferometer observatories with a goal of observing and understanding these GWs and the events that cause them [2]. In order to detect GWs, LIGO observatories must be able to detect changes in length in their 4 km arms many orders of magnitude smaller than the radius of a proton, and the smaller changes they are able to detect, the more GW events can be observed [3]. The current observatory design, called Advanced LIGO (aLIGO) has detected many GW events since the first observation in 2015, and improvements continue to be made on that design [2]. Soon, this design will reach the limits of its detection capabilities brought about by thermodynamics and quantum mechanics. In order to continue to improve detector sensitivity, a new upgrade is planned called "Voyager LIGO" which aims to increase the observation range 4-5 times and the detected event rate by a factor of 100 [4]. Voyager would operate at 123 K and use silicon mirrors to reduce thermo-elastic noise.

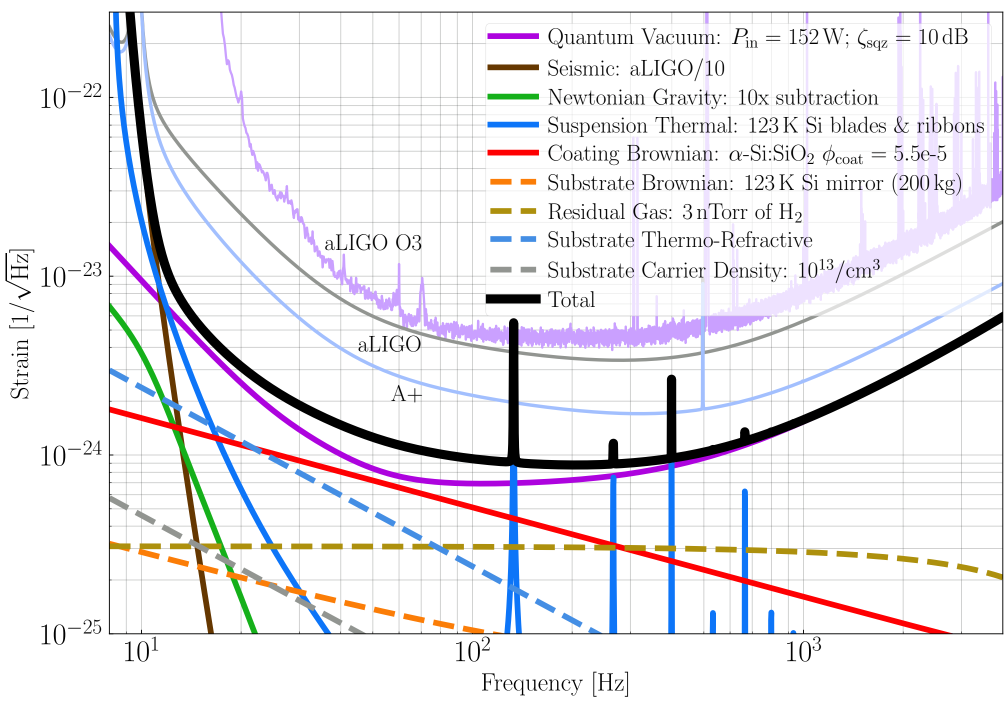

Figure 1: The target noise curve for LIGO Voyager as compared to noise curves for other LIGO designs. Figure from [4].

As can be seen in Figure 1, even for the Voyager design, the main source of noise for most detection frequencies is quantum noise, which arises due to random fluctuations in photon number travelling through the apparatus [5]. One parameter that sets a bound on quantum noise is the laser power circulating in each of the 4 km arms. Although aLIGO operates at a power of ∼750 kW in each of its arms, any increase in that number would allow for more quantum sensitivity. Because Voyager aims to operate at cryogenic temperatures, any increase in cavity laser power must have a corresponding increase in cooling of the end test mass in order to combat heating caused by absorption. Because LIGO observatories measure only one variable, the relative length of the arms, LIGO has been able to use "squeezed vacuum" injected into the interferometer to significantly decrease quantum noise [6]. However, the effectiveness of any quantum noise reduction is still limited by losses in interferometer optics. To combat this, a phase-sensitive optomechanical amplifier (PSOMA) has been proposed, which is capable of mitigating optical losses and reducing quantum noise [7]. Like the rest of the interferometer, the optics used for PSOMA must be kept at around 123 K because the device will use the same silicon mirrors as the rest of Voyager.

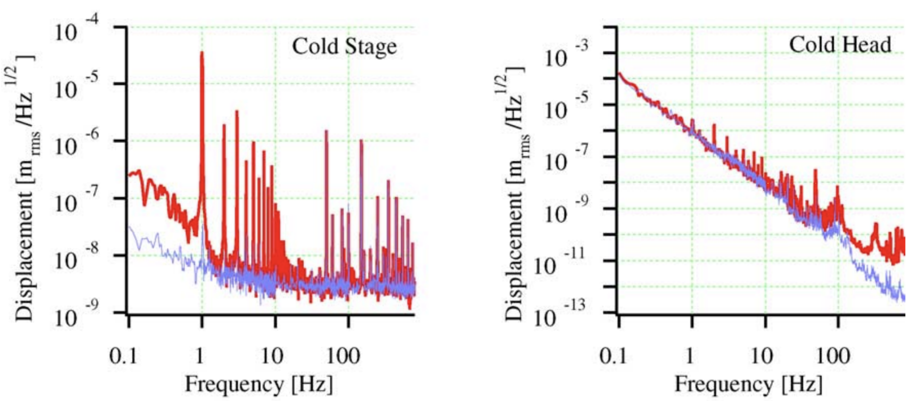

Figure 2: Vibration spectra for a 4 K pulse-tube cryocooler. The blue lines are the sensor noise while the red lines are the measured vibration in the cryocooler. The cold head and cold stage represent different parts of the cryocooler. Figure from [8].

Clearly, both of these ways of reducing quantum noise require cooling. Because any introduced vibration to the test mass would increase noise, cryocooling techniques must introduce little to no vibration to the system. Vibrations are also harmful near the test mass even if none of the vibration is transferred to it. This is because some laser light might be scattered off of the test mass onto surrounding objects before recombining with the main beam. If those objects are vibrating, a phase shift could be introduced along with fluctuations in radiation pressure, both of which would contribute to the noise [15]. Most cryocoolers cool by mechanically coupling the load to a cooling element which has some amount of vibration, which means that vibration would be introduced to the load. Figure 2 shows a vibration spectrum of a "low-vibration" cryocooler that was being looked at for other high sensitivity devices [8]. The vibration appears at some points negligible compared to the sensor noise, but the cold stage shows several peaks at harmonics of the 1 Hz fundamental and the cold head shows some measurable vibration above about 100 Hz, which is well within the detection bandwidth of LIGO. Figure 3 shows the maximum allowed displacement for the inner heat shield around the test mass. Comparing Figure 2 with Figure 3, we can clearly see that the vibrations of the cryocooler exceed those acceptable for the Voyager design. Although thermoelectric coolers can be vibration-free, they cannot operate at cryogenic temperatures and therefore are not an option. One potential solution to this problem is to use a solid-state

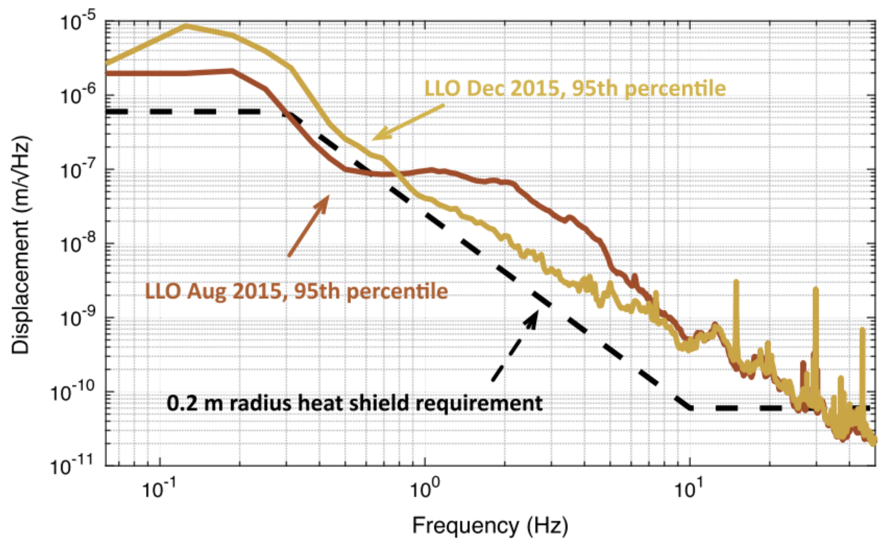

Figure 3: 95th percentile displacement spectra for LIGO Livingston and the maximum permitted displacement for the inner heat shield for the test mass. The inner heat shield is the object closest to the test mass. Figure from [15].

optical refrigerator to cool the interferometer, which is vibration free and can cool all the way to cryogenic temperatures.

1.2 Optical Refrigeration

The foremost method for optical refrigeration takes advantage of a quantum mechanical material phenomenon called anti-Stokes fluorescence, where the average fluorescence energy for a particular substance exceeds the average absorbed energy. To begin to understand this process, take the example a crystal doped with Yb^{3+}, the most common type of material used for optical refrigeration. Some other rare-earth (RE) ions exhibit similar behavior with only slightly different level structures, so this is a good model for all potential coolant materials [9]. When Yb^{3+} is embedded in its crystal field, its $^2F_{7/2}$ ground state and $^2F_{5/2}$ excited state manifolds split into 4 and 3 levels respectively due to a Stark shift [9], as shown on the left in Figure 4. In order to simplify the math and understanding of the process, a simpler four level model is used, as shown on the right in Figure 4. This model shows the relevant processes for optical refrigeration: pumped excitation, radiative decay, nonradiative decay, and thermalization within each manifold due to phonon absorption. For RE-doped crystals, the rethermalization rate is much faster than either decay rate, which allows the system to settle in an excited state quasi-equilibrium before decaying [9]. This is the origin of the anti-Stokes shift; some excited Yb^{3+} ions will thermalize into the $|3\rangle$ state before decaying either to the $|0\rangle$ or $|1\rangle$ state. Similarly, the ions which decay into $|0\rangle$ must thermalize into $|1\rangle$ before they can be pumped to the excited state.

If we assume the spin degeneracy of each level to be the same and apply Boltzmann statistics using the bulk temperature T of the crystal, we can arrive at expressions relating to the

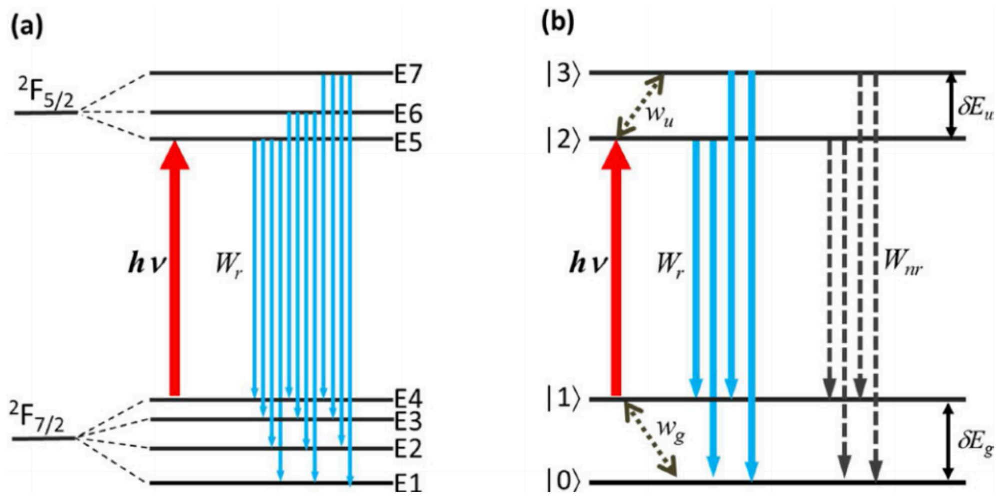

Figure 4: **(a)** The Stark-shifted level structure for Yb^{3+} showing all possible radiative decay processes, with the total rate of these processes being W_r, as well as the optical pumping at frequency ν. **(b)** A simplifed four-level model used to explain the cooling cycle for optical refrigeration, where the radiative and nonradiative decay rates are given by W_r and W_{nr} respectively. The phononic excitation rates are shown here as w_g for the ground state and w_u for the excited state. The width of the ground and excited state manifolds are given by δE_g and δE_u respectively. Figure from [9].

populations of each energy level for a system containing N_t ions, given by N_0, N_1, N_2, and N_3:

$$\frac{dN_1}{dt} = -\sigma_{12}\left(N_1 - N_2\right)\frac{I}{h\nu} + \frac{R}{2}\left(N_2 + N_3\right) - w_g\left(N_1 - N_0 e^{-\delta E_g/k_B T}\right), \tag{1}$$

$$\frac{dN_2}{dt} = \sigma_{12}\left(N_1 - N_2\right)\frac{I}{h\nu} - RN_2 + w_u\left(N_3 - N_2 e^{-\delta E_u/k_B T}\right), \tag{2}$$

$$\frac{dN_3}{dt} = -RN_3 - w_u\left(N_3 - N_2 e^{-\delta E_u/k_B T}\right), \tag{3}$$

$$N_0 + N_1 + N_2 + N_3 = N_t \tag{4}$$

where σ_{12} is the absorption cross-section for the $|1\rangle - |2\rangle$ transition, I is the irradiance of the pump laser, $R = 2\left(W_r + W_{nr}\right)$ is the total decay rate for the excited state, and k_B is the Boltzmann constant [9]. Additionally, we can arrive at an expression for the net power deposited to system by summing the absorbed power by the ions, the radiated power, and parasitically absorbed power as follows:

$$P_{net} = \sigma_{12}\left(N_1 - N_2\right) I - W_r\left[N_2\left(E_{21} + E_{20}\right) + N_3\left(E_{31} + E_{30}\right)\right] + \alpha_b I \tag{5}$$

where E_{xy} is the energy difference between $|x\rangle$ and $|y\rangle$, and α_b is the total parasitic absorption coefficient [9]. Next, we can write the absorption coefficient accounting for saturation by setting all of the time derivates equal to zero to find steady state behavior

$$\alpha = \frac{\alpha_0}{1 + I/I_s} \tag{6}$$

where

$$\alpha_0 = \sigma_{12} N_t \frac{e^{-\delta E_g/k_B T}}{1 + e^{-\delta E_g/k_B T}} \tag{7}$$

and

$$I_s = \frac{h\nu R}{\sigma_{12} Z_{gu}} \tag{8}$$

where $Z_{gu} \approx 1 + e^{-\delta E_g/k_B T}$[9]. Combining all of these, we get

$$P_{net} = \alpha I \left(1 - \eta_q \frac{h\nu_f}{h\nu}\right) + \alpha_b I, \tag{9}$$

where quantum efficiency $\eta_q = (1 + W_{nr}/W_r)^{-1}$ has been introduced and the mean fluorescence energy is given by

$$h\nu_f = h\nu + \frac{\delta E_g}{2} + \frac{\delta E_u}{1 + (1 + R/w_u)\, e^{\delta E_u/k_B T}} [9]. \tag{10}$$

P_{net}, being the net power deposited to the coolant, will be negative for a cooling system. This number as shown depends on both input light wavelength and temperature (in several places) so these parameters will have to be explored in order to optimize cooling power. The cooling power depends on several material parameters, including $R, w_{g,u}, \delta E_{g,u}, \sigma_{12}$ and α_b. For RE-doped systems, $R \ll w_{g,u}$, so differences in these two values can largely be ignored [9].

1.3 Past Experimental Results

In order to use an optical refrigerator, a thermal link must be established between the RE-doped cooling crystal and the load which needs to be cooled, among other setup requirements. To date, one fully solid-state optical cryocooler used to cool scientific equipment has produced publishable results [10]. The system cooled a room temperature HgCdTe sensor to 134.9 K in about 4 h. A block diagram of that refrigerator is shown in Figure 5. This cryocooler used YLF ($LiYF_4$) crystal doped with 10% YB^{3+} that had been shown to be able to reach sub-100 K temperatures when pumped by a 1020 nm laser [10]. In order to optimize the amount of light absorbed, the crystal was placed in a Herriott cell so that the light took 40 round trips before it left the cell. The doped YLF was bonded using a technique called "Adhesive-Free Bonding" to an undoped YLF thermal link with a high reflectance mirror at the end to shield the rest of the cooling system and the load from radiated heat from the crystal [10]. This mirror made thermal contact with a copper "coldfinger" which conducted the heat from the load to the crystal [10]. The whole system was mounted on a low conductivity silica aerogel support and placed inside a copper clamshell lined with low emissivity coating to minimize the amount of radiated power inside the refrigerator [10].

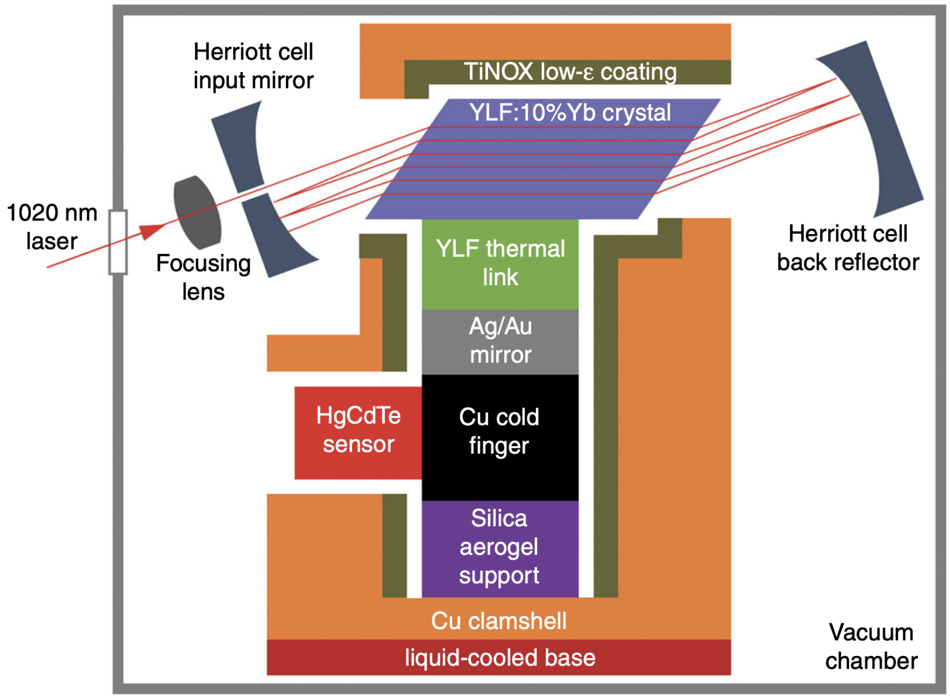

Figure 5: A block diagram showing the important parts of the first published optical cryocooler. Figure from [10].

A history of optical refrigeration results is shown in Figure 6. Early optical cooling experiments used fluorozirconate glasses like ZBLAN(P) as hosts due to the availability of high purity samples from their use for optical fibers in the telecommunications industry [9]. Since then, high purity YLF has emerged as the most common crystal host to be used for optical refrigerators for several reasons. First, YLF has a lower average phonon energy which decreases the likelihood of multiphonon emission which would contribute to nonradiative decay and lower quantum efficiency [11]. Additionally, it has a broad transparency range and relatively high thermal conductivity, both of which help with optimizing cooling power and efficiency [11].

Yb^{3+} has been the most common RE ion used in optical refrigeration experiments to date largely due to the availability of high power lasers in the appropriate wavelength range (∼1000 nm) [12]. However, other RE ions show promise in this area. Several years ago, optical cooling using Er^{3+} was lightly explored, but there has not been much progress on improving the efficiency Er^{3+}-doped systems to any practical level [9] [13]. Recently, YLF doped with Ho^{3+} and Tm^{3+} has shown early success in cooling experiments [14]. The intrigue of using these ions is that the relevant pumping transitions are about half the energy as those of Yb^{3+}. Using lower energy transitions can lead to higher cooling power if all other parameters are kept similar. The best way to understand this is by looking at Equation 9 and assuming that there is very little parasitic absorption and the quantum efficiency is near 1, as would have to be true in any usable optical refrigerator. This gives $P_{net} \sim \alpha I(h\nu - h\nu_f)/(h\nu)$. In general for optical coolants, the difference $h\nu_f - h\nu$ tends to be of order $k_B T$ independent of the pump energy scale due to that difference coming from rethermalization within the

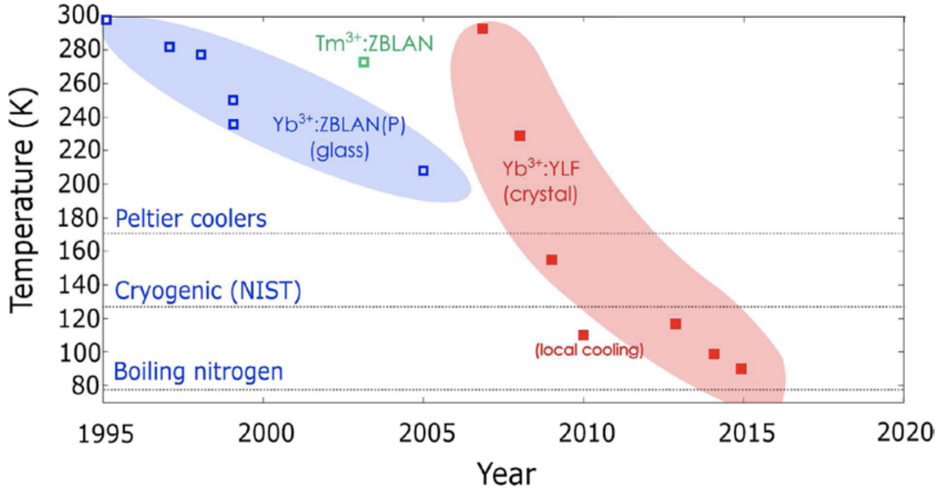

Figure 6: A history of optical refrigeration experimental results through 2015. Note the improvement in performance following the switch from ZBLAN(P) glass to YLF crystal. Figure from [9].

manifolds [16]. So this means that $P_{net} \propto -k_B T/(h\nu)$, meaning that a lower energy gap could lead to higher cooling power as long as parasitic absorption and nonradiative decay are still able to be minimized. However, ions with lower energy gaps are more prone to nonradiative decay because multiphonon emission probabilities increase exponentially with decreasing energy gap, though the rate of this exponential is highly dependent on the choice of host [16]. This means that low phonon energy would likely be especially important in hosts for low-energy gap ions.

For optical cooling to be useful for LIGO, a high-power refrigerator capable of cooling the relevant systems would have to be designed. Considerations will have to be made about the coolant material, the thermal coupling to the load, and the housing for such a system. To start, a prototype optical refrigerator must be designed to explore how the technique might be useful and demonstrate a proof of concept of cooling a load.

2 Objectives

The goal of this project is to begin to explore the viability of solid-state optical cooling for LIGO interferometers. The first step in the process is working toward a proof of concept demonstration of optically refrigerating a small (∼10-100 g) load. Although a lack of access to a laboratory is a challenge in this process, there are many goals that can be accomplished remotely. To start, the goal will be to identify an optical refrigerant as much potential cooling power as possible while only requiring a commercially available pump laser, likely in the 1-2 mm range. Then, other design considerations for the experiment must be made, including attempting to account for the radiation pressure of the pump laser and finding a way to thermally coupling the load to the coolant without absorbing any of its radiated energy. Another significant challenge will be shielding any cooled element from the high power radiation coming from the coolant crystal. In the end, the hope is to arrive at an experiment or prototype which accurately models how optical refrigeration could be used to cool LIGO optics. Ideally, some useful information to be able to get out of this prototype would be the cooling power at 123 K, the operating temperature of Voyager.

3 Approach

To begin, a literature review of recent advances in the field of optical refrigeration will be performed. The goal of this review is to identify viable materials for an optical refrigeration demonstration, ideally optimizing the cooling power possible with the material. Other important considerations for this literature review include the laser that would be required to cool the material and how easily one could acquire a crystal with the necessary purity. This review may require some calculation to find the cooling power at various temperatures from the data in those papers. Once a candidate material or candidate materials are found, experimental design would begin. Likely this will involve more reading of relevant literature to see techniques that have been used by other groups to take advantage of solid state cooling. This may also involve some calculations or light modeling to predict what would happen with particular setups. Additionally, modeling the radiation pressure of the pump laser may be necessary to see whether radiation pressure noise would have a significant impact on the noise budget. If all of this is successful, a next step could be to think through ways the prototype could be scaled up so that the technique may be used on the scales necessary to cool LIGO optics.

4 Project Schedule

- **Weeks 1-2:** Conduct literature review of relevant optical refrigeration papers to identify candidate coolant materials.
- **Weeks 3-6:** Design a setup to demonstrate optical refrigeration on a small load using the material identified in the first weeks. Here the methods for thermal coupling must be investigated.
- **Weeks 7-8:** Find ways to determine how the radiation pressure noise from the refrigerator pump laser might affect the noise floor of the relevant LIGO systems.
- **Weeks 9-end:** Explore and design ways that the demonstration might be improved in order to make optical cooling viable for use on LIGO instruments.

References

[1] https://www.ligo.caltech.edu/page/what-are-gw

[2] https://www.ligo.caltech.edu/page/about

[3] https://www.ligo.caltech.edu/page/ligos-ifo

[4] R.X. Adhikari et al., *A Cryogenic Silicon Interferometer for Gravitational-wave Detection*; arXiv:2001.11173.

[5] The LIGO Scientific Collaboration et al., *Advanced LIGO*; Class. Quantum Grav. **32** 074001 (2015).

[6] https://www.ligo.caltech.edu/mit/page/research-development;

[7] Y. Bai et al., *A phase-sensitive optomechanical amplifier for quantum noise reduction in laser interferometers*; arXiv:1909.02264.

[8] T. Tomaru et al., *Vibration analysis of cryocoolers*; Cryogenics **34** 309-317 (2004).

[9] D.V. Seletskiy et al., *Laser cooling in solids: advances and prospects*; Rep. Prog. Phys. **79** 096401 (2016).

[10] M.P. Hehlen et al., *First demonstration of an all-solid-state optical cryocooler*; Light: Science & Applications **7** 15 (2018).

[11] S. Bigotta et al., *Single fluoride crystals as materials for laser cooling applications*; Proc. SPIE **6461**, Laser Cooling of Solids (2007).

[12] M.P. Hehlen et al., *Solid-state Optical Refrigeration*; Handbook on the Physics and Chemistry of Rare-Earths **46** (2014).

[13] N.J. Condon et al., *Optical cooling in Er3+:KPb2Cl5*; Optics Express **17** 7 (2009).

[14] S. Rostami et al., *Optical refrigeration of Tm:YLF and Ho:YLF crystals* Proc. SPIE **9765**; Optical and Electronic Cooling of Solids (2016).

[15] B. Shapiro et al, *Cryogenically cooled ultra low vibration silicon mirrors for gravitational wave observatories*; Cryogenics **81** 83 (2017).

[16] C.W. Hoyt et al, *Observation of Anti-Stokes Fluorescence Cooling in Thulium-Doped Glass*; Phys. Rev. Lett. **85** 17 (2000).